

UC Irvine

UC Irvine Previously Published Works

Title

Critical current density and flux pinning in Zr_{0.96}V_{0.04}B₂ superconductor with AIB₂ structure

Permalink

<https://escholarship.org/uc/item/7x88x5kk>

Journal

Journal of Applied Physics, 114(13)

ISSN

0021-8979

Authors

Jung, Soon-Gil
Vanacken, J
Moshchalkov, VV
[et al.](#)

Publication Date

2013-10-07

DOI

10.1063/1.4821283

Copyright Information

This work is made available under the terms of a Creative Commons Attribution License, available at <https://creativecommons.org/licenses/by/4.0/>

Peer reviewed

Critical current density and flux pinning in $\text{Zr}_{0.96}\text{V}_{0.04}\text{B}_2$ superconductor with AlB_2 structure

Soon-Gil Jung,¹ J. Vanacken,¹ V. V. Moshchalkov,¹ S. T. Renosto,² C. A. M. dos Santos,² A. J. S. Machado,² Z. Fisk,³ and J. Albino Aguiar^{4,a)}

¹INPAC-Institute for Nanoscale Physics and Chemistry, KU Leuven, Celestijnenlaan 200D, B-3001 Leuven, Belgium

²Escolade Engenharia de Lorena, Universidade de São Paulo, P.O. Box 116, Lorena, SP, Brazil

³Department of Physics and Astronomy, University of California at Irvine, Irvine, California 92697, USA

⁴Departamentode Física, Universidade Federal de Pernambuco, 50670-901 Recife, PE, Brazil

(Received 23 May 2013; accepted 31 August 2013; published online 4 October 2013)

We have investigated the critical current density (J_c) and the flux pinning behavior in $\text{Zr}_{0.96}\text{V}_{0.04}\text{B}_2$ superconductor with an AlB_2 structure. V substitutions in Zr sites of non-superconducting ZrB_2 system lead to superconductivity, and the 4% V-substituted $\text{Zr}_{0.96}\text{V}_{0.04}\text{B}_2$ compounds show the highest superconducting transition temperature (T_c) of ~ 8.7 K. The magnetic hysteresis ($M-H$) loops for the $\text{Zr}_{0.96}\text{V}_{0.04}\text{B}_2$ demonstrate type-II superconducting behavior in a broad temperature range, and the J_c is estimated from the $M-H$ loops using the Bean model. The analysis of the double-logarithmic $J_c(H)$ plots indicates the dominance of collective pinning in $\text{Zr}_{0.96}\text{V}_{0.04}\text{B}_2$, and that $J_c(H)$ and magnetic field dependences of the flux pinning force density (F_p) are well fitted by the double exponential model which takes into account the existence of two superconducting gaps.

© 2013 AIP Publishing LLC. [<http://dx.doi.org/10.1063/1.4821283>]

I. INTRODUCTION

The discovery of the superconducting transition at ~ 40 K in MgB_2 has brought about great interest to materials with an AlB_2 structure (space group $P6/mmm$) because of their potential for having a high superconducting transition temperature (T_c).^{1,2} AlB_2 -type metal diborides, such as NbB_2 , ZrB_2 , TaB_2 , and so on, have been extensively studied, and a superconducting transition is observed in nonstoichiometric boride compounds such as MoB_{2+x} and NbB_{2+x} .³⁻⁷ In addition, AgB_2 and AuB_2 were predicted to have T_c higher than 50 K from the theoretical estimates,^{8,9} but recently much lower $T_c \sim 7$ K than theoretically predicted was found experimentally in AgB_2 thin films.¹⁰ It should also be noted that, despite a favorable prediction of their high T_c ,¹¹⁻¹⁴ it is difficult to synthesize these materials with an AlB_2 structure.

The presence of superconductivity in stoichiometric diboride compounds of TMB_2 (TM : Nb, Mo, Ta, Zr) is a controversial issue.¹⁵⁻¹⁷ On the other hand, boron rich MoB_{2+x} and NbB_{2+x} compounds and the Mo or the Nb substituted diboride compounds by other metals, such as $(\text{Mo}_{0.96}\text{Zr}_{0.04})_{0.88}\text{B}_2$, $\text{Mo}_{1-x}\text{M}_x\text{B}_{2.5}$ and $\text{Nb}_{1-x}\text{M}_x\text{B}_{2.5}$ (M : Sc, Zr, Y, V, Hf, etc.), and so on, clearly show the superconducting behavior with a stable AlB_2 structure.^{3-5,18} Among them, ZrB_2 is a very interesting material due to similar lattice parameters with MgB_2 and the possibility of the multiband superconductivity.^{19,20} However, a well defined superconducting transition was not yet observed in ZrB_2 , and the reported occurrence of superconductivity at 5.5 K in ZrB_2 polycrystals could be attributed to the presence of the dodecaboride ZrB_{12} phases as impurities in the samples.^{20,21} The

ZrB_{12} shows a superconductivity below ~ 6 K and has an UB_{12} structure.²²

Very recently, we have studied the effect of the V substitution for the Zr site in ZrB_2 compounds and found its favorable effect on T_c . Interestingly, a small percent of V substitution on the Zr sites induces superconductivity in a non-superconducting ZrB_2 , and 4% V-substituted $\text{Zr}_{0.96}\text{V}_{0.04}\text{B}_2$ compounds show a maximum T_c of ~ 8.7 K.²³ Moreover, basic properties of these compounds suggest a multiband behavior, and they have a high upper critical field ($H_{c2}(0)$) of ~ 16 T in spite of a low T_c , which make these material more interesting for further studies. The critical current density (J_c) is one of the important parameters of superconductor, but the research concerning J_c of the ZrB_2 with Zr substituted by V has not yet been carried out. In addition, the study on the J_c and flux pinning force for metal diboride superconductor with multigap except for MgB_2 is rarely reported, although they are very important factors for basic properties and real applications in superconductor.

In this paper, we report on the critical current density (J_c) and the flux pinning behavior of a new superconducting compound $\text{Zr}_{0.96}\text{V}_{0.04}\text{B}_2$ at various temperatures. The J_c is estimated from the magnetic hysteresis ($M-H$) loops using Bean's critical state model. We have found that collective pinning is dominant at most temperatures, and the field dependences of the J_c and the flux pinning force density are well fitted by the double exponential model consistent with the presence of two superconducting gaps.

II. EXPERIMENTS

The $\text{Zr}_{0.96}\text{V}_{0.04}\text{B}_2$ polycrystals with a typical size of $2 \times 3 \times 0.5$ mm³ were synthesized from high purity elements by using a Ti gettered arc furnace under Ar atmosphere. The sample was re-melted five times to improve its homogeneity

^{a)}Author to whom correspondence should be addressed. Electronic mail: albino@df.ufpe.br.

of the sample. The details of the fabrication and the basic properties for the $Zr_{1-x}V_xB_2$ compounds are described in Ref. 23. X-ray diffraction (XRD) and scanning electron microscopy (SEM) were used for the structural analysis for the $Zr_{0.96}V_{0.04}B_2$ samples after polishing to make a flat surface. The superconducting transition was measured resistively by the standard four-probe method and magnetically by a magnetic property measurement system (MPMS, Quantum Design). In order to investigate the critical current density (J_c) and the flux pinning force, the magnetization hysteresis ($M-H$) loops were measured by a vibrating sample magnetometer (VSM, Oxford Instruments).

III. RESULTS AND DISCUSSION

Figure 1 presents the $Zr_{0.96}V_{0.04}B_2$ XRD pattern, and in the inset SEM image for the polished sample. The XRD data present no diffraction peaks ascribable to impurities, and it is obtained that the lattice constants a -axis and c -axis are $a = 3.164 \text{ \AA}$ and $c = 3.524 \text{ \AA}$, respectively. The a -axis lattice constant of the $Zr_{0.96}V_{0.04}B_2$ is rarely changed compared to ZrB_2 , while the c -axis lattice constant is reduced by $\sim 1.7\%$,²³ which affects the electronic properties and eventually induce superconductivity. The SEM image of the polished $Zr_{0.96}V_{0.04}B_2$ sample, shown in the inset in Fig. 1, shows irregular grain sizes with clear grain boundaries. This microstructure could have an influence on flux pinning and critical current density.²⁴

Figure 2(a) presents a well defined superconducting transition of a new superconducting $Zr_{0.96}V_{0.04}B_2$ compound. The temperature dependences of its magnetization (M) were measured in a field of 0.5 Oe. The splitting of zero-field cooling (ZFC) and field cooling (FC) curves was observed at $\sim 8.7 \text{ K}$ and the ZFC shows a sharp transition, indicating the presence of bulk superconductivity. The inset of Fig. 2(a) gives the resistance as a function of temperature, which shows the T_c at $\sim 8.6 \text{ K}$ with the transition width ($\Delta T_c = T_{c,90\%} - T_{c,10\%}$) of about 0.4 K. The reason of a slightly lower T_c compared to T_c observed from the $M-T$ curve is probably due to the high applied current of 10 mA

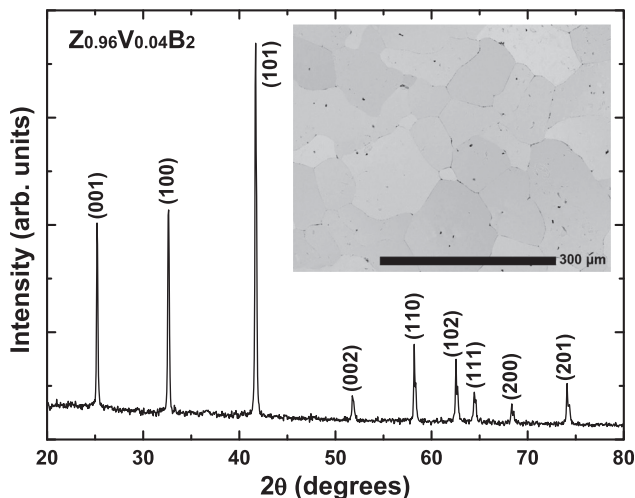


FIG. 1. XRD pattern of θ - 2θ scan for $Zr_{0.96}V_{0.04}B_2$ compound. Inset shows the SEM image for the polished sample.

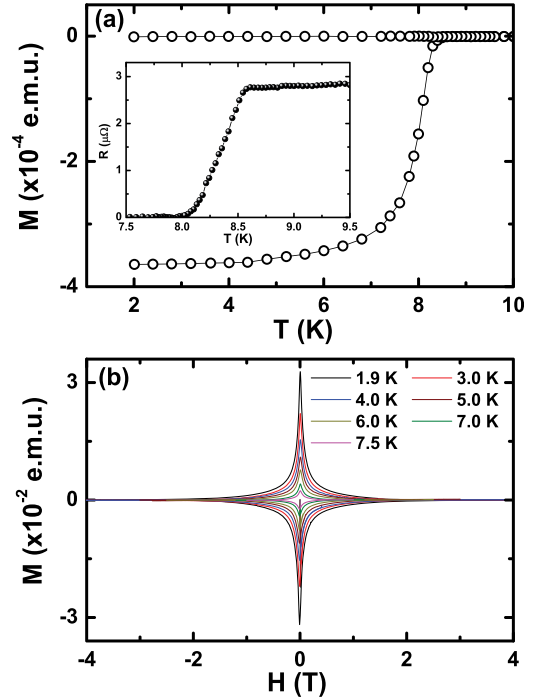


FIG. 2. (a) Temperature dependences of the magnetization (M) for $Zr_{0.96}V_{0.04}B_2$. Clear separation of ZFC and FC is observed at $\sim 8.7 \text{ K}$. The inset shows temperature dependence of the resistance in an applied current of 10 mA. (b) Magnetic hysteresis ($M-H$) loops at various temperatures for $Zr_{0.96}V_{0.04}B_2$. Magnetic field is applied from -5 to 5 T with a sweep rate of 0.2 T/min.

for the four-probe method which was needed due to very low resistance of the $Zr_{0.96}V_{0.04}B_2$. Magnetic hysteresis ($M-H$) loops were measured by a VSM with applied magnetic fields varying from -5 to 5 T with a sweep rate of 0.2 T/min over broad temperature range, which show obvious type-II superconducting $M-H$ curves, presented in Fig. 2(b).

The critical current density (J_c) for the $Zr_{0.96}V_{0.04}B_2$ was estimated from the $M-H$ loops using the Bean's critical state model with $J_c = 20\Delta M/[w(1 - w/3b)]$, where ΔM is the width of the $M-H$ loops as indicated in Fig. 2(b) and w

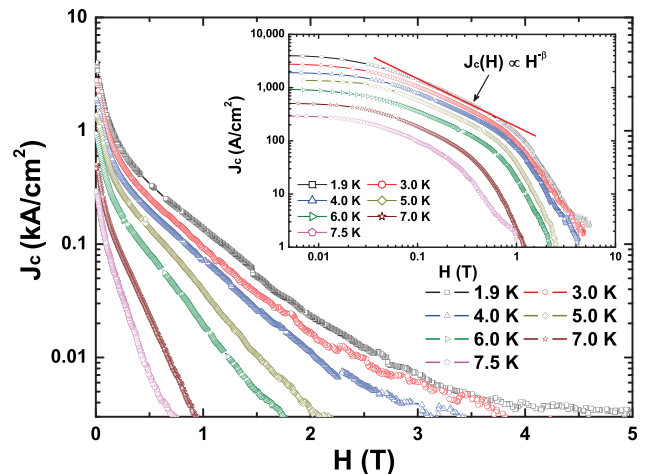


FIG. 3. Magnetic field dependences of the critical current density (J_c) at various temperatures for $Zr_{0.96}V_{0.04}B_2$, which demonstrate the exponential decrease. The inset presents the double-logarithmic graph for the $J_c(H)$ of $Zr_{0.96}V_{0.04}B_2$.

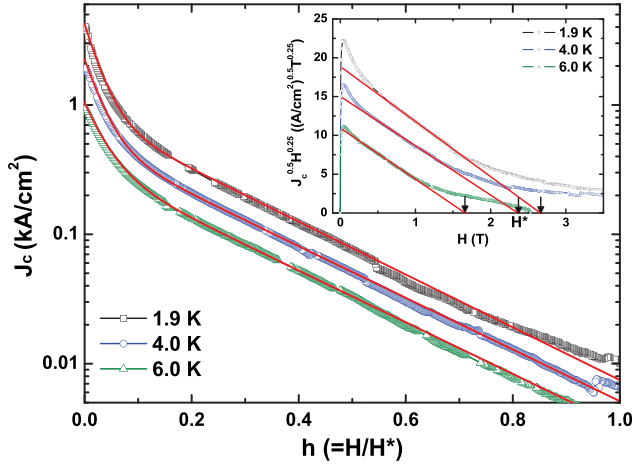


FIG. 4. Reduced field (h) dependences of the critical current density (J_c) for $Zr_{0.96}V_{0.04}B_2$. The solid lines are fitting curves by the double exponential model based on the presence of two superconducting gaps. The inset shows the Kramer plots to determine the irreversible fields (H^*), indicated by the arrows. The solid lines are fitting lines using the Kramer plots.

and b are the dimensions of the sample with $w < b$.^{25,26} The obtained magnetic field dependence of the J_c are presented in Fig. 3. The $J_c(H, T)$ is much lower than that of MgB_2 , for instance, $J_c(0)$ at 1.9 K is $\sim 4,000$ A/cm² for $Zr_{0.96}V_{0.04}B_2$ and is $\sim 10^6$ A/cm² for MgB_2 polycrystals.^{1,27} The low $J_c(0)$ of the $Zr_{0.96}V_{0.04}B_2$ is considered to be due to the poor electrically connectivity between the grains.²⁸ Furthermore, the irreversible regions lie at much lower fields than the upper critical fields, $H_{c2}(T)$, determined from the electrical transport measurement,²³ which is usually observed in high- T_c superconductors or in superconducting samples with weak pinning.^{29–31} The double-logarithmic plots for the $J_c(H)$ shown in the inset of Fig. 3 suggest that the pinning mechanism for the $Zr_{0.96}V_{0.04}B_2$ is probably associated with collective pinning, if one takes into account the power law $J_c(H) \propto H^{-\beta}$ in the slope regions indicated in Fig. 3 by the solid line.³² The values of the exponent β in the sloped regions are 0.85 ± 0.04 .

The exponential decrease in $J_c(H)$ has been reported for other superconducting materials,^{33,34} and the $J_c(H)$ for the new superconducting $Zr_{0.96}V_{0.04}B_2$ compound also shows the exponential decrease. The $J_c(H)$ curves over wide temperature regions for the $Zr_{0.96}V_{0.04}B_2$ can be well explained by using double exponential model associated with the two superconducting gaps, as shown in Fig. 4. This double exponential model is the stretched exponential function from a single exponential model in order to describe the $J_c(H)$ behavior of two-gap superconductor of MgB_2 .³⁵ The solid lines correspond to double exponential formula $J_c(h) = J_1 \exp(-A_1 h) + J_2 \exp(-A_2 h)$, where $h (=H/H^*)$ is the reduced field, A_1 and A_2 are constants, and J_1 and J_2 are partial critical current densities corresponding to the large and the small gap, respectively.^{33,35} Kramer plot of $J_c^{0.5} H^{0.25} \propto (H^* - H)$ has been used for evaluating empirical irreversible field (H^*), shown in the inset of Fig. 4. Only intermediate field regions with the linearity were used for the Kramer plots, and such sort of linearity is also observed in other multiband superconductors, like $PrPt_4Ge_{12}$ and MgB_2 .^{33,36,37}

Temperature dependences of all fitting parameters used in double exponential model are shown in Figs. 5(a) and 5(b). The temperature dependence of A_1 is roughly fitted by $(1 - t)$, indicated by the solid line. On the other hand, as shown in Fig. 5(a), A_2 is temperature independent having a constant value of 4.6 ± 0.1 for all temperatures studied. Figure 5(b) shows that J_1 and the J_2 are almost equal and present the same behavior with increasing temperature. Temperature dependence of the J_1 is similar with that of MgB_2 .³⁵ The inset of Fig. 5(b) presents the curves of each part of double exponential model, $J_c(h) = J_1 \exp(-A_1 h) + J_2 \exp(-A_2 h)$. The decreasing rate of the first parts is largely adjusted by the fitting parameter A_1 and these are merged at the point of $h = 0.195 \pm 0.002$, indicates that the small gap is probably to be almost suppressed at $h \approx 0.195$. On the other hand, the second parts are slightly separated at $h \approx 1$, due to broad non-linear regions at high fields in the Kramer plots.

Figure 6 shows the dependence of the normalized flux pinning force density, $f_p (=F_p/F_{p,max})$, on the reduced field, $h (=H/H^*)$, where F_p is the flux pinning force density and $F_{p,max}$ is the maximum F_p . The $f_p(h)$ curves are well scaled by using the double exponential model and the Kramer model of $f_p(h) \propto h^{0.5}(1-h)^2$ which are indicated in Fig. 6 by the solid and dashed lines, respectively. The scaling by the Kramer model, except for the deviations at $h > 0.6$, suggests the dominance of the strong pinning in the $Zr_{0.96}V_{0.04}B_2$, such as grain boundary and strong line pins,³⁸ however, it seems to contradict to the observed shape of the $M-H$ dependences because irreversible line is much low compared to H_{c2} . The double exponential model used for the $J_c(h)$

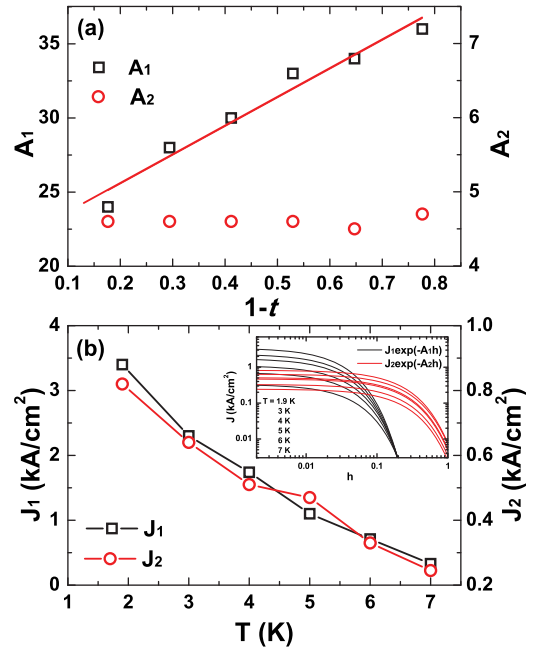


FIG. 5. Temperature dependences of the fitting parameters (a) A_1 and A_2 (b) J_1 and J_2 for double exponential model. A_1 is roughly proportional to the $(1 - t)$, where $t = T/T_c$, whereas $A_2 = 4.6 \pm 0.1$ regardless of temperature. Both fitting parameters J_1 and J_2 related to the size of critical current density show a similar temperature dependence. Inset of Fig. 5(b) shows the fitting curves for each exponential part in double exponential model, $J_1 \exp(-A_1 h)$ and $J_2 \exp(-A_2 h)$, where $h = H/H^*$.

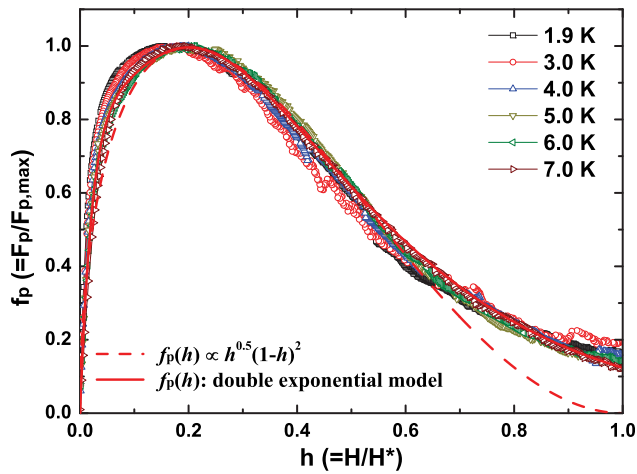


FIG. 6. Scaling behavior of the normalized flux pinning force density (f_p) as a function of reduced field (h) for $Zr_{0.96}V_{0.04}B_2$. The dashed line and the solid line are fitting curves obtained for strong pinning centers and two superconducting gaps, respectively.

fitting is quite good for scaling the $f_p(h)$ of the $Zr_{0.96}V_{0.04}B_2$, suggesting that two different superconducting gaps are indeed present in the $Zr_{0.96}V_{0.04}B_2$ system.

IV. CONCLUSIONS

In conclusion, we have investigated critical current density (J_c) and the flux pinning behavior in the new boride $Zr_{0.96}V_{0.04}B_2$ superconductor with an AlB_2 structure. The $J_c(H)$ is derived from the magnetic hysteresis ($M-H$) loops using Bean model in a broad temperature range, and it shows the dominance of collective pinning leading to the power law of $J_c(H) \propto H^{-\beta}$. The J_c 's in magnetic field show the exponential decrease, and the $J_c(H)$'s are well fitted by the double exponential model based on the presence of two superconducting gaps. In addition, reduced field dependences of the normalized flux pinning force density (f_p) are also well scaled by the double exponential model in comparison with a generally used model for flux pinning force scaling, such as Kramer model.

ACKNOWLEDGMENTS

The work at the KU Leuven was supported by the Methusalem Funding by the Flemish Government and by the FWO projects, Brazilian-Belgium cooperation project CNPq-FWO, under CNPq Grant Nos. 490297/2009-9 and 302892/2011-7, and by Brazilian agencies CAPES, CNPq, FACEPE (APQ-0589-1.05-08), and FAPESP (2011/05961-3).

¹C. Buzea and T. Yamashita, *Supercond. Sci. Technol.* **14**, R115 (2001).

²P. P. Singh, *Phys. Rev. Lett.* **87**, 087004 (2001).

³M. Mudgel, V. P. S. Awana, H. Kishan, I. Felner, Dr. G. A. Alvarez, and G. L. Bhalla, *J. Appl. Phys.* **105**, 07E313 (2009).

⁴M. Mudgel, V. P. S. Awana, G. L. Bhalla, and H. Kishan, *Solid State Commun.* **147**, 439 (2008).

- ⁵A. S. Cooper, E. Corenzwit, L. D. Longinotti, B. T. Matthias, and W. H. Zachariasen, *Proc. Natl. Acad. Sci. U.S.A.* **67**, 313 (1970).
- ⁶D. P. Young, R. G. Goodrich, P. W. Adams, J. Y. Chan, F. R. Fronczek, and L. L. Henry, *Phys. Rev. B* **65**, 180518 (2002).
- ⁷H. Rosner, W. E. Pickett, S.-L. Drechsler, A. Handstein, G. Behr, G. Fuchs, K. Nenkov, K.-H. Müller, and H. Eschrig, *Phys. Rev. B* **64**, 144516 (2001).
- ⁸S. K. Kwon, B. I. Min, S. J. Youn, and K. S. Kim, *J. Korean Phys. Soc.* **46**, L1295 (2005).
- ⁹F. Parvin, A. K. M. A. Islam, F. N. Islam, A. F. M. A. Wahed, and M. E. Haque, *Physica C* **390**, 16 (2003).
- ¹⁰R. Tomita, H. Koga, T. Uchiyama, and I. Iguchi, *J. Phys. Soc. Jpn.* **73**, 2639 (2004).
- ¹¹L. Leyarovska and E. Leyarovski, *J. Less-Common Met.* **67**, 249 (1979).
- ¹²B. Post, F. W. Glaser, and D. Moskowicz, *Acta Metall.* **2**, 20 (1954).
- ¹³P. Vajeeston, P. Ravindran, C. Ravi, and R. Asokamani, *Phys. Rev. B* **63**, 045115 (2001).
- ¹⁴C. A. Nunes, D. Kaczorowski, P. Rogl, M. R. Baldissera, P. A. Suzuki, G. C. Coelho, A. Grytsiv, G. André, F. Boureé, and S. Okada, *Acta Mater.* **53**, 3679 (2005).
- ¹⁵D. Kaczorowski, A. J. Zaleski, O. J. Zogal, and J. Klamut, "Incipient superconductivity in TaB_2 ," e-print [arXiv:0103571v2](https://arxiv.org/abs/0103571v2) (unpublished).
- ¹⁶A. Yamamoto, C. Takao, T. Masui, M. Izumi, and S. Tajima, *Physica C* **383**, 197 (2002).
- ¹⁷I. R. Shein and A. L. Ivanovskiĭ, *Phys. Solid State* **44**, 1833 (2002).
- ¹⁸L. E. Muzzy, M. Avdeev, G. Lawes, M. K. Haas, H. W. Zandbergen, A. P. Ramirez, J. D. Jorgensen, and R. J. Cava, *Physica C* **382**, 153 (2002).
- ¹⁹C. Jariwala, A. Chainani, S. Tsuda, T. Yokoya, S. Shin, Y. Takano, K. Togano, S. Otani, and H. Kito, *Phys. Rev. B* **68**, 174506 (2003).
- ²⁰V. A. Gasparov, N. S. Sidorov, and I. I. Zver'kova, *Phys. Rev. B* **73**, 094510 (2006).
- ²¹V. A. Gasparov, N. S. Sidorov, I. I. Zver'kova, and M. P. Kulakov, *JETP Lett.* **73**, 532 (2001).
- ²²Y. Wang, R. Lortz, Y. Paderno, V. Filippov, S. Abe, U. Tutsch, and A. Junod, *Phys. Rev. B* **72**, 024548 (2005).
- ²³S. T. Renosto, H. Consoline, C. A. M. dos Santos, J. Albino Aguiar, Soon-Gil Jung, J. Vanacken, V. V. Moshchalkov, Z. Fisk, and A. J. S. Machado, *Phys. Rev. B* **87**, 174502 (2013).
- ²⁴P. Mikheenko, E. Martínez, A. Bevan, J. S. Abell, and J. L. MacManus-Driscoll, *Supercond. Sci. Technol.* **20**, S264 (2007).
- ²⁵M. Imai, M. Akaiishi, and I. Shirovani, *Supercond. Sci. Technol.* **20**, 832 (2007).
- ²⁶S. Soltanian, M. J. Qin, S. Keshavarzi, X. L. Wang, and S. X. Dou, *Phys. Rev. B* **68**, 134509 (2003).
- ²⁷Q. Li, G. D. Gu, and Y. Zhu, *Appl. Phys. Lett.* **82**, 2103 (2003).
- ²⁸T. Matsushita, M. Kiuchi, A. Yamamoto, J.-i. Shimoyama, and K. Kishio, *Supercond. Sci. Technol.* **21**, 015008 (2008).
- ²⁹D. N. Zheng, H. D. Ramsbottom, and D. P. Hampshire, *Phys. Rev. B* **52**, 12931 (1995).
- ³⁰M. Willemin, C. Rossel, J. Hofer, H. Keller, A. Erb, and E. Walker, *Phys. Rev. B* **58**, R5940 (1998).
- ³¹G. Fuchs, K. Nenkov, G. Krabbes, R. Weinstein, A. Gandini, R. Sawh, B. Mayes, and D. Parks, *Supercond. Sci. Technol.* **20**, S197 (2007).
- ³²B. Dam, J. M. Huijbregtse, F. C. Klaassen, R. C. F. van der Geest, G. Doornbos, J. H. Rector, A. M. Testa, S. Freisem, J. C. Martinez, B. Stäubli-Pümpin, and R. Griessen, *Nature (London)* **399**, 439 (1999).
- ³³L. S. Sharath Chandra, M. K. Chattopadhyay, and S. B. Roy, *Supercond. Sci. Technol.* **25**, 105009 (2012).
- ³⁴K. J. Song, J. R. Thompson, M. Yethiraj, D. K. Christen, C. V. Tomy, and D. McK. Paul, *Phys. Rev. B* **59**, R6620 (1999).
- ³⁵J. Wang, Z. X. Shi, H. Lv, and T. Tamegai, *Physica C* **445**, 462 (2006); **449**, 104 (2006).
- ³⁶D. C. Larbalestier, L. D. Cooley, M. O. Rikel, A. A. Polyanskii, J. Jiang, S. Patnaik, X. Y. Cai, D. M. Feldmann, A. Gurevich, A. A. Squitieri, M. T. Naus, C. B. Eom, E. E. Hellstrom, R. J. Cava, K. A. Regan, N. Rogado, M. A. Hayward, T. He, J. S. Slusky, P. Khalifah, K. Inumaru, and M. Haas, *Nature (London)* **410**, 186 (2001).
- ³⁷P. Badica, T. Kondo, T. Kudo, Y. Nakamori, S. Orimo, and K. Togano, *Appl. Phys. Lett.* **85**, 4433 (2004).
- ³⁸E. J. Kramer, *J. Appl. Phys.* **44**, 1360 (1973).

Journal of Applied Physics is copyrighted by the American Institute of Physics (AIP). Redistribution of journal material is subject to the AIP online journal license and/or AIP copyright. For more information, see <http://ojps.aip.org/japo/japcr/jsp>